J|A|C|S COMMUNICATIONS

Published on Web 01/12/2010

Visualizing the Reaction Coordinate of an O-GlcNAc Hydrolase

Yuan He,[†] Matthew S. Macauley,[‡] Keith A Stubbs,[‡,§] David J Vocadlo,[‡] and Gideon J Davies*[,†]

York Structural Biology laboratory, Department of Chemistry, The University of York, YO10 5YW, U.K., Department of Chemistry, Simon Fraser University, 8888 University Drive, Burnaby, Canada, and Chemistry M313, School of Biomedical, Biomolecular and Chemical Sciences, University of Western Australia, 35 Stirling Highway, Crawley, Western Australia 6009, Australia

Received October 12, 2009; E-mail: davies@ysbl.york.ac.uk

O-GlcNAc[1] is a dynamic post-translational modification critical to life at the cellular level. Critical roles[1] for *O*-GlcNAc in the stress response, signal transduction, and transcriptional regulation[2] including polycomb repression[3,4] have been forwarded while dysregulation of *O*-GlcNAc has been implicated in type II diabetes[5] and neurodegeneration.[6,7] The partial reciprocity of *O*-GlcNAc with serine and threonine phosphorylation[8] is notable in view of its biological importance. Interestingly, in contrast to phosphorylation where over 600 enzymes are involved in catalyzing its addition and removal, only two enzymes regulate the *O*-GlcNAc modification in metazoans: *O*-GlcNAc transferase (OGT) and *O*-GlcNAc hydrolase (OGA).[1] The dynamic nature of the *O*-GlcNAc modification has made inhibitors of these two enzymes useful for altering cellular levels of *O*-GlcNAc and interrogating the biological roles of this modification. Small molecule chemical intervention has been particular successful with OGA,[9] a glycoside hydrolase family from GH84 (one of >110 sequence based families of glycoside hydrolases (www.cazy.org)). OGA catalyzes the removal of *O*-GlcNAc using a substrate-assisted catalytic mechanism. Here we define the reaction coordinate using chemical approaches and directly observe both the Michaelis complex and the oxazoline intermediate.

The 3-D structures of two close bacterial homologues of human OGA, NagJ[10] from *Clostridium perfringens* and *Bacteroides thetaiotaomicrometer Bt*GH84,[11] have had their 3-D structures determined (reviewed in ref 12). Together with enzymatic data,[11,13] these structures have solidified that both human and bacterial enzymes use a catalytic mechanism in which the *N*-acetyl carbonyl group is critical to catalysis, an indication of a two-step neighboring group reaction mechanism that proceeds through a bicyclic oxazoline intermediate, Figure 1. The 3-D structures revealed an active-center constellation of two adjacent carboxylates, which is a signature motif of the growing set of glycoside hydrolases harnessing neighboring group participation.[12] In the case of *Bt*GH84, in the first step of the reaction, "cyclization", D243 plays the role of general acid to aid departure of the leaving group while D242 activates the 2-acetamido group for nucleophilic attack; the net result of these coordinated processes is formation of the oxazoline intermediate, Figure 1. In the second step, "ring-opening", D243 acts as a general base to aid attack of a water molecule at the anomeric center while D242 aids opening of the oxazoline ring to form the product with retained stereochemistry at the anomeric center. To date, no analysis defining the complete set of stable species along the reaction coordinate of any GH family known to use substrate assisted catalysis (GH18, 20, 25, 56, 84, and 85)[12] has been presented. In general, such structural elucidation of species along the coordinates of enzyme catalyzed reactions

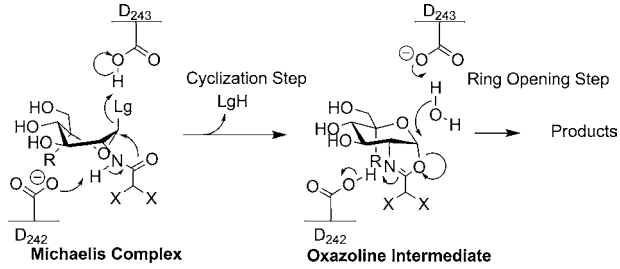

Figure 1. The catalytic mechanism of human OGA and family 84 glycoside hydrolases proceeds via a two-step reaction mechanism though a Michaelis complex shown here to have a distorted $^{1,4}B/^{1}S_3$ conformation and an oxazoline intermediate having a $^{4}C_1$ conformation. The catalytic residue numbering shown is for *Bt*GH84. For compound **1** (see Figure 2), R = H and X = F; for **2**, R = F and X = H; and for **3**, R = X = H.

is a difficult but illuminating process, motivated by a desire to enhance the basic understanding of enzyme catalysis and also serving to stimulate the design of highly potent inhibitors (for a recent perspective see ref 14).

A key species that defines the reaction coordinate of any enzyme-catalyzed reaction is the Michaelis complex. Various approaches to trap glycoside hydrolases with their unhydrolyzed substrates have included nonhydrolyzable or slowly turned over substrates and/or enzyme variants in which critical components of the catalytic apparatus have been compromised.[15] Recently a detailed linear free energy analysis of human OGA demonstrated that when a substrate contains a modest leaving group as well as a poor nucleophile, the catalytic efficiency of the enzyme is synergistically impaired.[16] We reasoned that, under the right conditions, such a substrate might be trapped in the active site unhydrolyzed. To this end, we tested a wide range of such substrates and obtained co-crystals of *Bt*GH84 and 3,4-difluorophenyl 2-deoxy-2-difluoroacetamido-β-D-glucopyranoside[16] **1** (details of synthesis are in the Supporting Information, SI online), Figure 2.

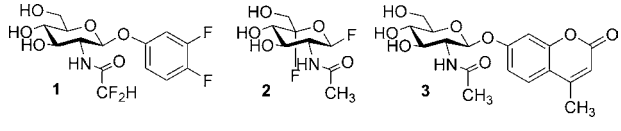

Figure 2. Compounds used in the visualization of the O-GlcNAcase reaction coordinate. (**1**) 3,4-Difluorophenyl 2-deoxy-2-difluoroacetamido-β-D-glucopyranoside, (**2**) 2-acetamido-2-deoxy-5-fluoro-β-D-glucopyranosyl fluoride, and (**3**) 4-methylumbelliferyl 2-acetamido-2-deoxy-β-D-glucopyranoside.

We solved the 3-D structure at 2.2 Å resolution (methods in SI, refinement statistic in Supplemental Table 1) harnessing the 2-fold noncrystallographic symmetry to reveal an unambiguous density for unhydrolyzed **1** within the active site, Figure 3a. Strikingly,

[†] The University of York.
[‡] Simon Fraser University.
[§] University of Western Australia.

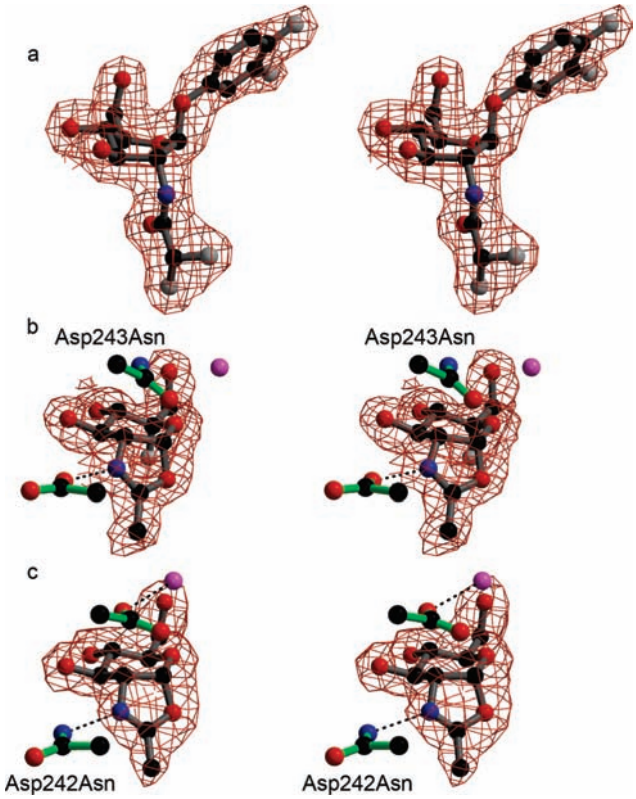

Figure 3. Visualization of the reaction coordinate of *O*-GlcNAc hydrolases. (a) Michaelis complex of **1** (shown with gray bonds) bound within the wild-type *Bt*GH84 glycoside hydrolase active site. (b) The 5F-oxazoline intermediate obtained from treating D243N *Bt*GH84 with **2**. The oxazoline intermediate obtained from treating D242N *Bt*GH84 with **3**. Electron densities are maximum likelihood weighted $2F_{obs} - F_{calc}$ synthesis contoured (approximately 0.4 $e^-/Å^3$) in divergent stereo.

the pyranose ring of the substrate adopts a conformation between $^{1,4}B$ and $^1S_3$, Figure 1, differing significantly from the $^4C_1$ conformation preferred in solution but consistent with trapped Michaelis complexes on GH18 chitinases[17] and GH20 chitobiases[18] that also share the neighboring group mechanism.[12] The distorted conformation we observe here, however, is consistent with work conducted on other glycosidases that act on a β-glycosidic linkage via a retaining catalytic mechanism involving formation of a covalent glycosyl enzyme intermediate.[15] Such a conformation places the leaving group C1−OR bond in a pseudoaxial position "above" the plane of the pyranose ring. As a result, the *N*-acetyl carbonyl oxygen of the substrate itself lies poised to displace the leaving group from the tetrahedral anomeric center, with an O_{nuc}−C1 distance of 3.4 Å and an O_{nuc}−C1−O_{lg} angle of 170° (Supplemental Movie 1).

Direct observation of enzyme bound intermediates has also proven difficult. For glycoside hydrolases, different approaches have been used to trap covalent glycosyl enzyme intermediates.[19] A bicylic oxazoline intermediate has never been observed, however, for any glycoside hydrolase using substrate-assisted catalysis, perhaps because these species are extremely reactive or perhaps because they are noncovalently bound to these enzymes. To surmount this problem and visualize the putative bicylic oxazoline intermediate we devised two different strategies. In the first strategy we used 2-acetamido-2-deoxy-5-fluoro-β-D-glucopyranosyl fluoride[20] **2**, Figure 2, since we speculated that the electronegative fluorine substituent adjacent to the endocyclic oxygen (O5) would slow both the formation and breakdown of the oxazoline intermediate by destabilizing the flanking cationic transition states. By analogy with other glycosidase systems, it was reasoned that incorporation of a very good fluoride leaving group would make the intermediate kinetically accessible and make the breakdown of the oxazoline intermediate relatively slow.[15,19] Despite these considerations, turnover of the putative 5-fluoro-2′-methyl-α-D-glucopyrano-[2,1-d]-Δ2′-oxazoline (5F-oxazoline) intermediate by the wild-type enzyme was likely too rapid and we were unable to observe this species by X-ray crystallography. Instead, we used **2** in conjunction with a variant of *Bt*GH84 in which the general acid/base is impaired (D243N) (Figure 1). We anticipated that the absence of the general acid/base would leave the cyclization step unaffected since departure of the fluoride ion leaving group cannot benefit from general acid catalysis. The ring-opening of the intermediate, however, would be slowed since the attack of water on the anomeric center is promoted by general base catalysis. This strategy succeeded and enabled accumulation and observation of the oxazoline in soaked and flash-frozen crystals, Figure 3b. We find the 5F-oxazoline intermediate binds in an approximate $^4C_1$ conformation.

The second strategy enabled us to observe a chemically "unmodified" oxazoline intermediate. A comparison of the set of GH families using substrate assisted catalysis reveals two key residues: a general acid/base (here D243) and a second group which also likely serves as a general acid/base to aid formation and breakdown of oxazoline intermediate (here D242), Figure 1. In all families except GH85, this second residue, that interacts directly with the oxazoline intermediate, is an Asp or Glu; however, it was recently shown that in GH85 an Asn can also support catalysis. Notably, these GH85 enzymes are efficient catalysts for biosynthesis, and this may be due to the oxazoline intermediate being more stable and favoring partitioning to acceptor sugars more efficiently than to water. With this in mind, we speculated that the analogous D242N variant of BtGH84 might retain activity but that the ring-opening step of the reaction may be slowed preferentially.

Specifically, we considered that departure of a fairly good phenol leaving group might still be fairly efficient but that breakdown of the oxazoline might be slower. Steady-state kinetics (Supporting Information) using a substrate with a 4-methylumbelliferone leaving group, namely **3**, showed that the D242N mutant was active on this substrate, albeit with an efficiency ~320-fold times lower than that of wild-type enzyme. At a pH value of 8.5 we find a 12-fold reduction in apparent K_m (1 mM to 0.08 mM, SI Figure 1), suggesting that the second step of the reaction may be the rate-determining step for this mutant enzyme (since $K_m = [E][S]/\sum[E\text{-bound species}]$, a low K_m suggests accumulation of an enzyme bound intermediate). In this scenario, departure of the activated leaving group enables cyclization to form the oxazoline intermediate, but breakdown of the intermediate by ring-opening is slow since protonation of the oxazoline either on enzyme by D242N or in solution is likely not thermodynamically favorable. This hypothesis predicts that presteady state stopped flow fluorescence kinetics should reveal a burst phase arising from accumulation of the oxazoline intermediate followed by a steady state turnover of this species. We find precisely such kinetic behavior occurring when the enzyme is initially mixed with the substrate, Figure 4a. Further consistent with this hypothesis is that the magnitude of the burst matched the enzyme concentration (burst size is 94% of $[E]_o$). Accordingly, when we soaked crystals of the D242N variant grown at pH 8.5 with **3**, we observe an intact trapped oxazoline intermediate. Like the 5F-oxazoline, the unsubstituted oxazoline binds in a $^4C_1$ chair conformation, Figure 3c. Indeed, beyond a slight shift in the position of Lys166 away from the O3 atom of the D242N oxazoline complex that likely reflects the elevated pH used

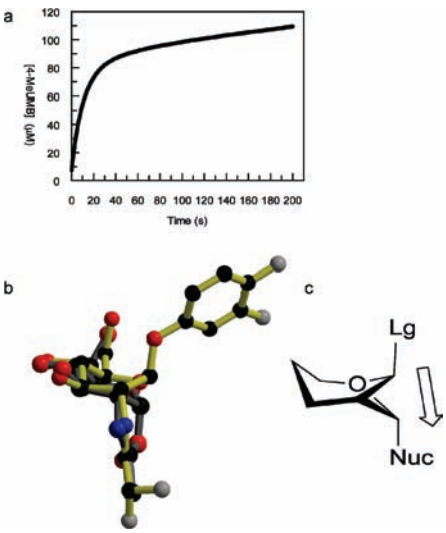

Figure 4. Electrophilic migration[21] along the reaction coordinate of *O*-GlcNAc hydrolases. (a) Presteady state kinetics for the hydrolysis of **3** with the D242N variant at pH 8.5. (b) Overlap of the D242N trapped oxazoline intermediate (gray) overlaid with the Michaelis complex of unhydrolysed **1**. (c) Simplified schematic representation of the "electrophilic migration" of the anomeric carbon from the Michaelis complex ($^{1,4}B/^{1}S_3$ conformation) through to the oxazoline intermediate in the $^{4}C_1$ conformation.

for this experiment, we observe that this oxazoline and the D243N 5F-oxazoline complex bind with essentially identical interactions in the active center. Notably, the oxazoline ring itself is stabilized through sandwiching between the aromatic planes of Trp337 and Tyr282 with the oxazoline nitrogen and oxygen hydrogen bonding with Asp242 and Asn339 respectively (Supplemental Figure 2). In both trapped intermediates a potential hydrolytic water (colored purple in Figure 3b,c) lies ~3.6 Å above the anomeric carbon poised for nucleophilic attack.

Together, the Michaelis complex revealing the pyranose ring adopts a $^{1}S_3$ skew boat conformation and the oxazoline intermediate showing a $^{4}C_1$ chair conformation point to a $^{1}S_3 \leftrightarrow {}^{4}H_3 \leftrightarrow {}^{4}C_1$ conformational itinerary that defines the reaction coordinate for the formation of the oxazoline intermediate. As is clearly demonstrated through an overlap of the Michaelis and oxazoline complexes (Figure 4b), such a pathway is an exemplar of what Schramm has described as an "electrophilic migration"[21] mechanism in which the anomeric carbon follows a pathway migrating from bonded contact with the leaving group "above" the plane of the pyranose ring to bonded contact with the waiting nucleophile "below" the plane with only minimal motion of other substrate atoms (Figure 4c).[15] Recent metadynamic studies have revealed that the $^{1}S_3$ conformation not only is a local free-energy minimum but also is "pre-activated" for in-line nucleophilic attack, and in the case of the β-D-*gluco* configuration,[22] this conformation maximizes the charge distribution across the C1−O1 bond, lengthening this bond while minimizing the O5−C1 distance, features that all favor the electrophilic migration of C1 through the transition state. Interestingly, we find that the thiazoline analogue, which is a potent transition state analogue and has been proposed to emulate the transition state, binds quite similarly to *Bt*GH84 as do the oxazolines. The C1−S bond (1.85 Å), which is longer than the C1−O bond (1.45 Å), places the C1 carbon of the thiazoline ~0.2 Å closer to the position of C1 in the Michaelis complex than the C1 of the oxazoline reaction intermediate. Such observations are consistent with Whitworth's proposal made for human OGA that a broad high energy series of species encompassing a late transition state are found along the reaction coordinate.[23] The description of a $^{1}S_3 \leftrightarrow {}^{4}H_3 \leftrightarrow {}^{4}C_1$ pathway for oxazoline formation, presented here, coupled to solution studies on OGA transition-state poise[23] therefore provides the first sighting of an oxazoline intermediate bound to any glycoside hydrolase using substrate assisted catalysis and coherently defines the conformational itinerary of this class of enzymes.

Acknowledgment. This work was funded by the Biotechnology and Biological Sciences Research Council (BBSRC) and the Canadian Institutes of Health Research and the Natural Sciences and Engineering Research Council of Canada (NSERC). G.J.D. is a Royal Society-Wolfson Research Merit award recipient. D.J.V. is a Canada Research Chair in chemical glycobiology and a Scholar of the Michael Smith Foundation for Health Research (MSFHR). M.S.M. holds scholarships from NSERC and the MSFHR.

Supporting Information Available: Details of organic synthesis of compound **1**, structure solution and refinement and steady and presteady-state kinetics. Movie of the Michaelis complex of BtGH84 with **1** and schematic diagram of interactions of the compound **3** derived oxazoline intermediate. This material is available free of charge via the Internet at http://pubs.acs.org.

References

(1) Hart, G. W.; Housley, M. P.; Slawson, C. *Nature* **2007**, *446*, 1017–1022.
(2) Fujiki, R.; Chikanishi, T.; Hashiba, W.; Ito, H.; Takada, I.; Roeder, R. G.; Kitagawa, H.; Kato, S. *Nature* **2009**, *459*, 455–U179.
(3) Sinclair, D. A. R.; Syrzycka, M.; Macauley, M. S.; Rastgardani, T.; Komljenovic, I.; Vocadlo, D. J.; Brock, H. W.; Honda, B. M. *Proc. Natl. Acad. Sci. U.S.A.* **2009**, *106*, 13427–13432.
(4) Gambetta, M. C.; Oktaba, K.; Muller, J. *Science* **2009**, *325*, 93–96.
(5) Dentin, R.; Hedrick, S.; Xie, J. X.; Yates, J.; Montminy, M. *Science* **2008**, *319*, 1402–1405.
(6) Liu, F.; Iqbal, K.; Grundke-Iqbal, I.; Hart, G. W.; Gong, C. X. *Proc. Natl. Acad. Sci. U.S.A.* **2004**, *101*, 10804–10809.
(7) Yuzwa, S. A.; Macauley, M. S.; Heinonen, J. E.; Shan, X.; Dennis, R. J.; He, Y.; Whitworth, G. E.; Stubbs, K. A.; McEachern, E. J.; Davies, G. J.; Vocadlo, D. J. *Nat. Chem. Biol.* **2008**, *4*, 483–490.
(8) Wang, Z.; Gucek, M.; Hart, G. W. *Proc. Natl. Acad. Sci. U.S.A.* **2008**, *105*, 13793–13798.
(9) Macauley, M. S.; Vocadlo, D. J. *Biochim. Biophys. Acta* **2009**, http://dx.doi.org/10.1016/j.bbagen.2009.07.028.
(10) Rao, F. V.; Dorfmueller, H. C.; Villa, F.; Allwood, M.; Eggleston, I. M.; van Aalten, D. M. *EMBO J.* **2006**, *25*, 1569–1578.
(11) Dennis, R. J.; Taylor, E. J.; Macauley, M. S.; Stubbs, K. A.; Turkenburg, J. P.; Hart, S. J.; Black, G.; Vocadlo, D. J.; Davies, G. J. *Nat. Struct. Mol. Biol.* **2006**, *13*, 365–371.
(12) Martinez-Fleites, C.; He, Y.; Davies, G. J. *Biochim. Biophys. Acta* **2009**, http://dx.doi.org/10.1016/j.bbagen.2009.07.019.
(13) Macauley, M. S.; Whitworth, G. E.; Debowski, A. W.; Chin, D.; Vocadlo, D. J. *J. Biol. Chem.* **2005**, *280*, 25313–25322.
(14) Schwartz, S. D.; Schramm, V. L. *Nat. Chem. Biol.* **2009**, *5*, 551–558.
(15) Vocadlo, D.; Davies, G. J. *Curr. Opin. Chem. Biol.* **2008**, *12*, 539–555.
(16) Greig, I. R.; Macauley, M. S.; Williams, I. H.; Vocadlo, D. J. *J. Am. Chem. Soc.* **2009**, *131*, 13415–13422.
(17) van Aalten, D. M. F.; Komander, D.; Synstad, B.; Gaseidnes, S.; Peter, M. G.; Eijsink, V. G. H. *Proc. Natl. Acad. Sci. U.S.A.* **2001**, *98*, 8979–8984.
(18) Tews, I.; Perrakis, A.; Oppenheim, A.; Dauter, Z.; Wilson, K. S.; Vorgias, C. E. *Nat. Struct. Biol.* **1996**, *3*, 638–648.
(19) Rempel, B. P.; Withers, S. G. *Glycobiology* **2008**, *18*, 570–586.
(20) Stubbs, K. A.; Scaffidi, A.; Debowski, A. W.; Mark, B. L.; Stick, R. V.; Vocadlo, D. J. *J. Am. Chem. Soc.* **2008**, *130*, 327–335.
(21) Fedorov, A.; Shi, W.; Kicska, G.; Fedorov, E.; Tyler, P. C.; Furneaux, R. H.; Hanson, J. C.; Gainsford, G. J.; Larese, J. Z.; Schramm, V. L.; Almo, S. C. *Biochemistry* **2001**, *40*, 853–860.
(22) Biarnes, X.; Ardevol, A.; Planas, A.; Rovira, C.; Laio, A.; Parrinello, M. *J. Am. Chem. Soc.* **2007**, *129*, 10686–10693.
(23) Whitworth, G. E.; Macauley, M. S.; Stubbs, K. A.; Dennis, R. J.; Taylor, E. J.; Davies, G. J.; Greig, I. R.; Vocadlo, D. J. *J. Am. Chem. Soc.* **2007**, *129*, 635–644.

JA9086769